

# Parallel Predictive Entropy Search for Multi-objective Bayesian Optimization with Constraints

Eduardo C. Garrido-Merchán  
 Universidad Autónoma de Madrid  
 eduardo.garrido@uam.es

Daniel Hernández-Lobato  
 Universidad Autónoma de Madrid  
 daniel.hernandez@uam.es

## Abstract

Real-world problems often involve the optimization of several objectives under multiple constraints. An example is the hyper-parameter tuning problem of machine learning algorithms. In particular, the minimization of the estimation of the generalization error of a deep neural network and at the same time the minimization of its prediction time. We may also consider as a constraint that the deep neural network must be implemented in a chip with an area below some size. Here, both the objectives and the constraint are black boxes, *i.e.*, functions whose analytical expressions are unknown and are expensive to evaluate. Bayesian optimization (BO) methodologies have given state-of-the-art results for the optimization of black-boxes. Nevertheless, most BO methods are sequential and evaluate the objectives and the constraints at just one input location, iteratively. Sometimes, however, we may have resources to evaluate several configurations in parallel. Notwithstanding, no parallel BO method has been proposed to deal with the optimization of multiple objectives under several constraints. If the expensive evaluations can be carried out in parallel (as when a cluster of computers is available), sequential evaluations result in a waste of resources. This article introduces PPESMOC, Parallel Predictive Entropy Search for Multi-objective Bayesian Optimization with Constraints, an information-based batch method for the simultaneous optimization of multiple expensive-to-evaluate black-box functions under the presence of several constraints. Iteratively, PPESMOC selects a batch of input locations at which to evaluate the black-boxes so as to maximally reduce the entropy of the Pareto set of the optimization problem. To our knowledge, this is the first batch method for constrained multi-objective BO. We present empirical evidence in the form of synthetic, benchmark and real-world experiments that illustrate the effectiveness of PPESMOC.

## 1 Introduction

Black-boxes are defined as functions whose analytical expression is unknown. Hence, we can not compute their gradients. Moreover, these are expensive to evaluate functions, either in terms of computational time or other resources. Additionally, the evaluations of these functions are noisy. That is, the evaluation of these functions is contaminated by noise. More precisely, an example of a black-box is the hyper-parameter tuning of a machine learning algorithm (Feurer and Hutter, 2019). In this problem, the estimation of the generalization error carried out by a machine learning algorithm over a dataset is minimized. Furthermore, many real-world scenarios involve the simultaneous optimization of a set of objectives subject to several constraints being simultaneously validated. An example of such an scenario is tuning the control system of a four-legged robot. We may be interested in finding the optimal control parameters to minimize the robot’s energy consumption and maximize locomotion speed (Ariizumi et al., 2014), under the constraint that the amount of weight placed on a leg of the robot does not exceed a specific value, or similarly, that the maximum angle between the legs of the robot is below some other value for safety reasons. Measuring the objectives and the constraints in this case may involve

an expensive computer simulation or doing some actual experiment with the robot. There is no analytical expression to describe the output of that process, which can take a significant amount of time. Moreover, the result of the experiment can be different each time, depending, *e.g.*, on the environmental conditions.

Bayesian optimization (BO) has been empirically shown to be a good class of methods to deal with the optimization problems described in the previous paragraph (Mockus et al., 1978). In particular, several constrained multi-objective BO methods have obtained good results in that setting (Feliot et al., 2017; Garrido-Merchán and Hernández-Lobato, 2019). These methods iteratively suggest, in an intelligent way, a point at which to evaluate the objectives and the constraints to solve the optimization problem in a small number of steps. This process is repeated until enough points have been evaluated. Then, a recommendation is made as the potential solution of the problem. However, a limitation of BO methods for constrained multi-objective optimization is that they choose a single location at a time at which to evaluate the black-boxes (Garrido-Merchán and Hernández-Lobato, 2019). Assume that a cluster of computers or some other resource is available to perform the evaluation of the black-boxes at several points in parallel. If only a single point is evaluated each time, this results in a waste of resources and leads to sub-optimal optimization results. The problem described can be solved by using BO methods that suggest not only a single point at which to evaluate the black-boxes, but a batch or collection of points of adjustable size (Azimi et al., 2012; Bergstra et al., 2011; González et al., 2016; Shah and Ghahramani, 2015).

To the best of our knowledge, no BO method has been proposed to deal with the optimization of multiple objectives under several constraints, when the evaluations can be done in parallel. Only sequential methods have been introduced to tackle the constrained multi-objective scenario (Feliot et al., 2017; Garrido-Merchán and Hernández-Lobato, 2019). Therefore, the literature about BO is missing important methods to address BO problems with the characteristics described. In this work, we propose a BO method called PPESMOC, Parallel Predictive Entropy Search for Multi-objective Bayesian Optimization with Constraints, that can precisely address the problems described. Specifically, such a method can suggest, at each iteration, a batch of points at which to evaluate all the black-boxes in parallel. The method proposed is based on an extension of the PESMOC (Predictive Entropy Search for Multi-objective Bayesian Optimization with Constraints) method (Garrido-Merchán and Hernández-Lobato, 2019) and an extension of parallel single-objective and un-constrained BO (Shah and Ghahramani, 2015).

A batch or parallel BO method usually consists of a probabilistic surrogate model that provides a predictive distribution of the black-box function and an acquisition function whose maximum indicates the next batch of points to be evaluated. In particular, the acquisition function of the BO method that we consider in this work receives as an input a batch of candidate input locations at which to perform the evaluation of the black-boxes in parallel and estimates the expected reduction in the entropy of the solution of the optimization problem. The difference with PESMOC is that here, the acquisition function evaluates a batch of points instead of a single point. However, as we will see in the following sections, considering the suggestion of a batch of points is challenging and leads to several problems that need to be tackled by a novel methodology, which is precisely what the PPESMOC acquisition function represents.

Summing up, in this research work we present the first method for multi-objective BO with constraints that allows for parallel evaluations. We believe that this is an important contribution for the BO community. Furthermore, we provide an exhaustive and detailed empirical evaluation of such a method in several optimization problems. We also compare results with some simple base-lines to address such a problem, showing that our approach sometimes leads to better results. Importantly, however, PPESMOC scales better with the batch size than these simple methods. This allows to consider bigger batch sizes.

The rest of the paper is organized as follows: Section 2 describes in detail the fundamentals of BO and, in particular, constrained multi-objective parallel or batch BO. Then, Section 3 describes the proposed approach, PPESMOC, and how to compute an approximate acquisition function that suggests a batch of points based on the expected reduction of the entropy of the Pareto set. After that, Section 4 includes related work that describes batch BO methods and BO methods that can address multi-objective problems with constraints. Then, Section 5 contains extensive

experiments to evaluate the performance of PPESMOC in synthetic, benchmark and real-world optimization problems. We have compared results with a base-line which chooses the points to evaluate at random and with a simple method that applies iteratively a sequential BO method for constrained multi-objective BO (as many times as the batch size). This last method introduces virtual observations (fantasies) to avoid choosing many times the same point to be evaluated. The results show that PPESMOC performs better than a random search strategy and similarly or better than sequential base-lines. The advantage of PPESMOC is, however, that its cost scales much better with respect to the batch size than the sequential base-lines. Finally, Section 6 enumerates the conclusions of this article.

## 2 Constrained Multi-Objective Parallel Bayesian Optimization

After introducing the parallel constrained multi-objective BO scenario, this section formalizes the described problem and the BO algorithm adapted to this scenario. Recall that in Section 3 we will describe our proposed approach, PPESMOC, so here we will only focus on general parallel constrained multi-objective BO concepts that need to be understood before.

As it was described in the previous section, the purpose of BO is to retrieve the extremum  $\mathbf{x}^*$  of a black-box function  $f(\mathbf{x})$  where  $\mathbf{x} \in \mathcal{X}$  and  $\mathcal{X}$  is the input space where  $f(\mathbf{x})$  can be evaluated. Formally, we seek to obtain  $\mathbf{x}^*$  such that,

$$\mathbf{x}^* = \arg \min_{\mathbf{x} \in \mathcal{X}} f(\mathbf{x}), \quad (1)$$

assuming minimization. However, in this work, we consider the problem of simultaneously minimizing  $K$  functions  $f_1(\mathbf{x}), \dots, f_K(\mathbf{x})$  which we define as objectives, subject to the non-negativity of  $C$  constraints  $c_1(\mathbf{x}), \dots, c_C(\mathbf{x})$ , over some bounded domain  $\mathcal{X} \in \mathbb{R}^d$ , where  $d$  is the dimensionality of the input space. The problem considered is:

$$\min_{\mathbf{x} \in \mathcal{X}} f_1(\mathbf{x}), \dots, f_K(\mathbf{x}) \quad \text{s.t.} \quad c_1(\mathbf{x}) \geq 0, \dots, c_C(\mathbf{x}) \geq 0. \quad (2)$$

We say that a point  $\mathbf{x} \in \mathcal{X}$  is feasible if  $c_j(\mathbf{x}) \geq 0, \forall j$ , that is, it satisfies all the constraints. This leads to the concept of feasible space  $\mathcal{F} \subset \mathcal{X}$ , that is the set of points that are feasible. In this scenario, only the solutions contained in  $\mathcal{F}$  are considered valid.

Focusing on the multi-objective optimization part of the problem, most of the times it is impossible to optimize all the objective functions at the same time, as they may be conflicting. For example, in the control system of the robot described before, most probably maximizing locomotion speed will lead to an increase in the energy consumption. In spite of this, it is still possible to find a set of optimal points  $\mathcal{X}^*$  known as the *Pareto set* (Siarry and Collette, 2003). More formally, we define that the point  $\mathbf{x}$  dominates the point  $\mathbf{x}'$  if  $f_k(\mathbf{x}) \leq f_k(\mathbf{x}') \forall k$ , with at least one inequality being strict. Then, the Pareto set is the subset of non-dominated points in  $\mathcal{F}$ , the feasible space, which is equivalent to this expression  $\forall \mathbf{x}^* \in \mathcal{X}^* \subset \mathcal{F}, \forall \mathbf{x} \in \mathcal{F} \exists k \in 1, \dots, K$  such that  $f_k(\mathbf{x}^*) < f_k(\mathbf{x})$ . The Pareto set is considered to be optimal because for each point in that set one cannot improve in one of the objectives without deteriorating some other objective. Given  $\mathcal{X}^*$ , a final user may then choose a point from this set according to their preferences, *e.g.*, locomotion speed vs. energy consumption.

To solve efficiently the previous problems, *i.e.*, find the Pareto set in  $\mathcal{F}$  with a small number of evaluations, BO methods perform a sequence of steps iteratively. The number of iterations is delimited by the budget that an user can afford to evaluate the black-boxes, which is assumed to be costly. For example, the user may only be able to test 50 configurations of a machine learning algorithm. In this case, the number of BO iterations would be 50. At each iteration  $t$ , a point  $\mathbf{x}_t$  is suggested. The point  $\mathbf{x}_t$  is suggested by following the next steps: first, BO methods fit a probabilistic model, typically, a Gaussian process (GP) to the observed data of each black-box function (objective or constraint). The uncertainty about the potential values of these functions

given by the predictive distribution of the GPs is then used to build an acquisition function  $\alpha(\mathbf{x})$  whose maximum determines the next point to be evaluated. An acquisition function  $\alpha(\mathbf{x})$  represents an exploration-exploitation trade-off. Specifically, the acquisition function  $\alpha(\mathbf{x})$  favors exploration in the sense that it is high in areas where no point  $\mathbf{x}$  has been evaluated before. These areas may contain values near the optimum value. It also needs to perform exploitation, *i.e.*, the acquisition function  $\alpha(\mathbf{x})$  favors the evaluation of points that are likely to lead to good evaluations. Concretely, we expect that the new evaluations are near the current best observed value, as we assume that the function is smooth. Importantly, a constrained multi-objective acquisition function takes into account the predictive distribution of every black-box (Garrido-Merchán and Hernández-Lobato, 2019).

Considering the sequential scenario, the maximum of the acquisition function  $\alpha(\mathbf{x})$  indicates the most promising location at which to evaluate next the objectives  $f_1(\mathbf{x}), \dots, f_K(\mathbf{x})$  and the constraints  $c_1(\mathbf{x}), \dots, c_C(\mathbf{x})$  to solve the optimization problem at each iteration  $t$ . Namely,

$$\mathbf{x}_t = \arg \max_{\mathbf{x} \in \lambda} \alpha_t(\mathbf{x}), \quad (3)$$

The process of evaluating the black-boxes, updating the probabilistic models, and generating the acquisition function is repeated iteratively. After enough observations have been collected like this, the probabilistic models can be optimized to provide an estimate of the Pareto set of the original problem. Importantly, the acquisition function  $\alpha(\mathbf{x})$  only depends on the uncertainty provided by the probabilistic models and not on the actual objectives or constraints. This means that it can be evaluated and optimized very quickly to identify the next evaluation point.

By carefully choosing the points at which to evaluate the objectives and the constraints, BO methods find a good estimate of the solution of the optimization problem in a small number of evaluations (Brochu et al., 2010; Shahriari et al., 2015). We can see in Figure 1 an unconstrained single-objective example of the steps performed by a BO method. In this figure, the acquisition function  $\alpha(\mathbf{x})$  is plotted on green, the GP posterior distribution on blue, observations are represented as black dots and the latest observation is represented as a red dot. The ground truth is plotted as a dashed black line, the GP posterior mean as a continuous black line and the GP posterior uncertainty of its prediction as a blue area, surrounding the mean. The GP posterior uncertainty represents one standard deviation of the predictive distribution around the mean. We can see how the GP predictive distribution  $p(f(\mathbf{x})|\mathcal{D})$  and the acquisition function  $\alpha(\mathbf{x})$  shapes change at each iteration  $t$ .

The process described is repeated iteratively until the budget of evaluations  $T$  is consumed. Finally, BO recommends the point  $\mathbf{x}$  whose observation value  $y$  has been the best as the solution of the problem. In particular, the goodness of a solution of a constrained multi-objective problem can be measured in terms of the hyper-volume metric (Hernández-Lobato et al., 2016). Concretely, assuming minimization, the hyper-volume is simply the volume above the feasible Pareto frontier  $\mathcal{Y}$  (*i.e.*, the function values associated to the feasible Pareto set  $\mathcal{F}$ ), which is maximized by the actual Pareto set. We can see in Figure 2 a visual representation of the constrained multi-objective scenario. The figures at the top represent the two objectives and the constraint involved in the optimization problem. The figures below represent the feasible Pareto set  $\mathcal{F}$  and its associated Pareto frontier  $\mathcal{Y}$ . The hyper-volume will be the region contained above the Pareto frontier with respect to a reference point, which is usually set as the worst result for each objective. To sum up, we enumerate the described steps in Algorithm 1.

The following sections will explain in detail the GP models used to describe each black-box and the fundamentals of parallel BO, where not only one but a batch of points are suggested at each iteration  $t$ .

## 2.1 Modeling the Black-boxes Using Gaussian Processes

We model each objective  $f_k(\cdot)$  and constraint  $c_j(\cdot)$  using a Gaussian process (GP) (Rasmussen, 2003). A Gaussian Process (GP) is a collection of random variables (of potentially infinite size), any finite number of which have (consistent) joint Gaussian distributions. Equivalently, it describes

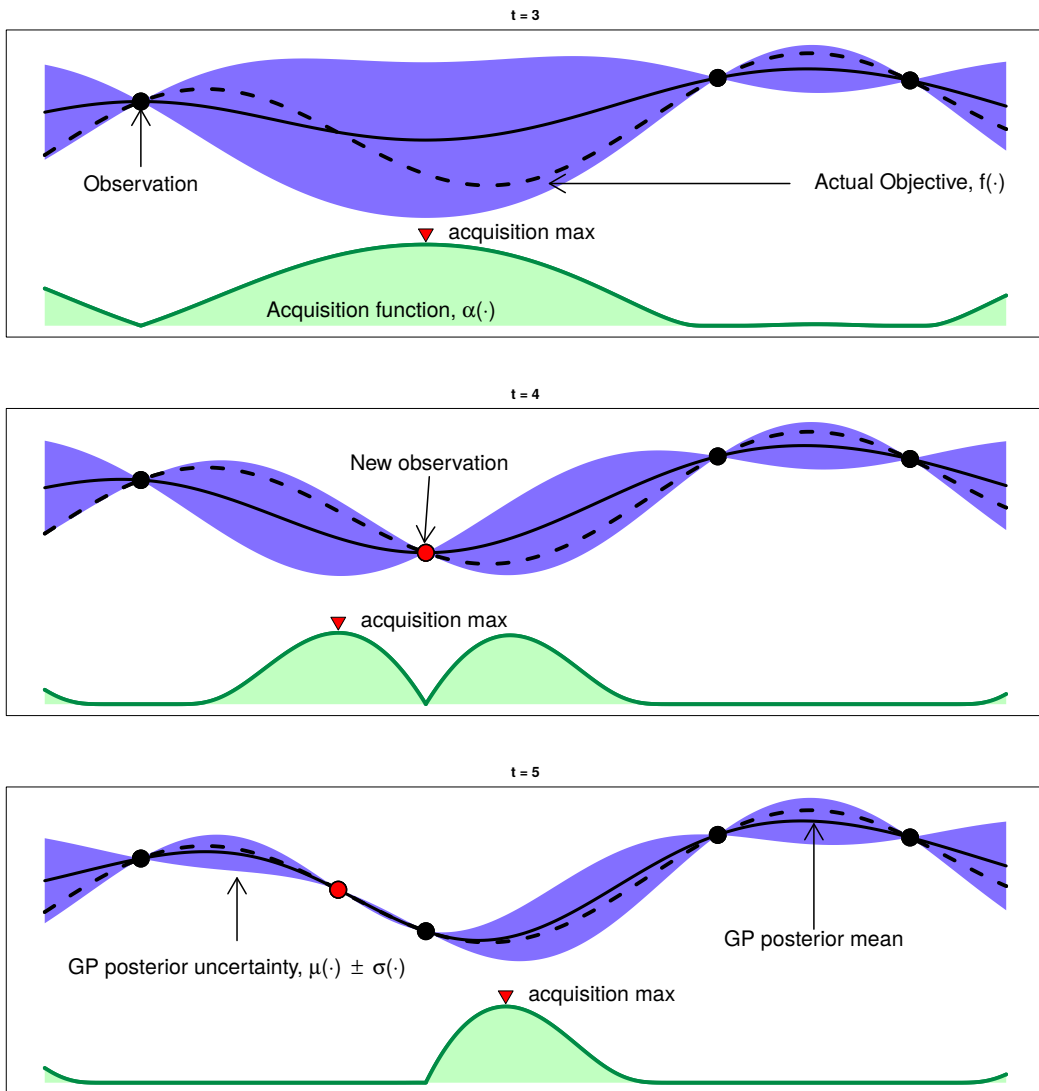


Figure 1: BO acquisition function  $\alpha(\mathbf{x})$  and GP predictive distribution  $p(f(\mathbf{x})|\mathcal{D})$  on a toy 1D noiseless problem. The figures show a GP estimation of the objective  $f(\mathbf{x})$  over three iterations. The acquisition function  $\alpha(\mathbf{x})$  is shown in the lower part of the plot. The acquisition  $\alpha(\mathbf{x})$  is high where the GP predicts a low value of the objective  $f(\mathbf{x})$  and where the uncertainty about its prediction is high. Those regions in which it is unlikely to find the global minimum  $\mathbf{x}^*$  of  $f(\mathbf{x})$  have low acquisition values, and will not be explored.

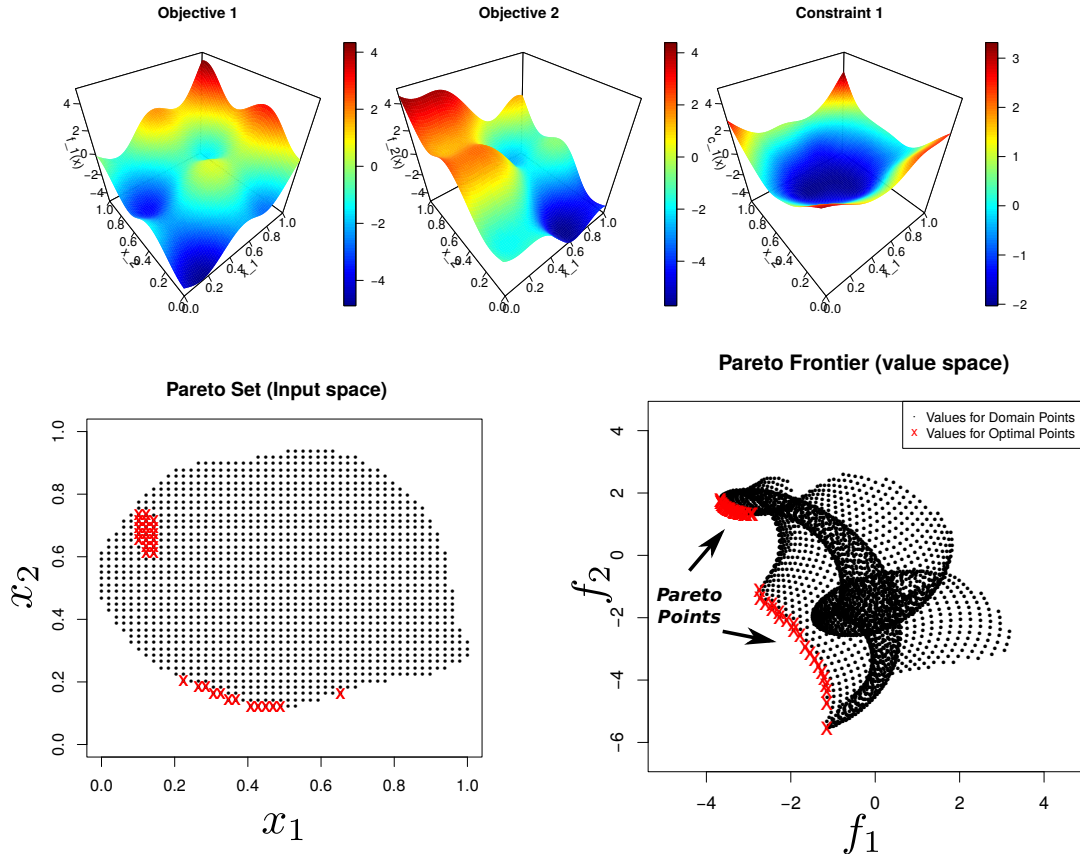


Figure 2: Constrained multi-objective optimization problem with two objectives and one constraint. (Top) Shapes of the objectives and constraints of the constrained multi-objective optimization problem. (Bottom, left) Feasible space represented by black dots and feasible Pareto set represented by red dots. (Bottom, right) Associated values of the feasible space represented by black dots and Pareto frontier represented by red dots.

a stochastic process whose values, at any finite number of input locations, have joint Gaussian distributions. We can also think of GPs as defining a distribution over functions where inference takes place directly in the space of functions (Rasmussen, 2003). A GP can also be defined as a distribution over functions, *i.e.*, we can sample functions from it. So, if we assume that each of the black-boxes  $f(\cdot)$  is a sample of the GP, it is reasonable to use a GP to model the black-box in BO given that it is a non-parametric flexible model, it is easy to estimate its hyper-parameters and it is a robust model that is not expected to over-fit with small amounts of data.

More formally, a GP is fully characterized by a zero mean and a covariance function or kernel  $k(\mathbf{x}, \mathbf{x}')$ , that is,  $f(\mathbf{x}) \sim \mathcal{GP}(\mathbf{0}, k(\mathbf{x}, \mathbf{x}'))$ . The covariance function of the GP receives two points as an input,  $\mathbf{x}$  and  $\mathbf{x}'$ . We define the prior mean function  $m(\mathbf{x})$  and the covariance function  $k(\mathbf{x}, \mathbf{x}')$  that computes the covariance between  $f(\mathbf{x})$  and  $f(\mathbf{x}')$  as:

$$\begin{aligned} m(\mathbf{x}) &= \mathbb{E}[f(\mathbf{x})], \\ k(\mathbf{x}, \mathbf{x}') &= \mathbb{E}[(f(\mathbf{x}) - m(\mathbf{x}))(f(\mathbf{x}') - m(\mathbf{x}'))]. \end{aligned} \quad (4)$$

We assume independent GPs for each black-box function, objective or constraint. Consider the observations of a particular black-box function  $\{(\mathbf{x}_i, y_i)\}_{i=1}^N$ , where  $y_i = f(\mathbf{x}_i) + \epsilon_i$ , with  $f(\cdot)$  the

**Input:** Maximum number of evaluations  $T$ .  
**for**  $t = 1, 2, 3, \dots, T$  **do**  
    **1: if**  $N = 1$ :  
        Choose  $\mathbf{x}_t$  at random from  $\mathcal{X}$ .  
    **else:**  
        Find  $\mathbf{x}_t$  by maximizing the acquisition function:  $\mathbf{x}_t = \arg \max_{\mathbf{x} \in \mathcal{X}} \alpha_t(\mathbf{x})$ .  
    **2:** Evaluate the black-boxes  $f_1(\mathbf{x}), \dots, f_K(\mathbf{x})$  and  $c_1(\mathbf{x}), \dots, c_C(\mathbf{x})$  at  $\mathbf{x}_t$ :  
         $y_t = f_k(\mathbf{x}_t) + \epsilon_t$ .  
    **3:** Augment the dataset of each black-box with the new observation:  
         $\mathcal{D}_{1:t} = \mathcal{D}_{1:t-1} \cup \{\mathbf{x}_t, y_t\}$ .  
    **4:** Fit again the GP models using the augmented dataset  $\mathcal{D}_{1:t}$ .  
**end**  
**5:** Obtain the recommendation  $\mathbf{x}^*$ : Point associated with the value that optimizes the hyper-volume of the Pareto frontier or with the best observed value.  
**Result:** Recommended point  $\mathbf{x}^*$

**Algorithm 1:** BO of a constrained multi-objective problem with objectives  $f_1(\mathbf{x}), \dots, f_K(\mathbf{x})$  and constraints  $c_1(\mathbf{x}), \dots, c_C(\mathbf{x})$ .

black-box function and  $\epsilon_i$  some Gaussian noise. A GP gives a distribution for the potential values of  $f(\cdot)$  at a new set of input points  $\mathbf{X}^* = (\mathbf{x}_1^*, \dots, \mathbf{x}_B^*)^T$  of size  $B$ . Let  $\mathbf{f}^* = (f(\mathbf{x}_1^*), \dots, f(\mathbf{x}_B^*))^T$ . The predictive distribution for  $\mathbf{f}^*$  is Gaussian.  $p(\mathbf{f}^* | \mathbf{y}) = \mathcal{N}(\mathbf{f}^* | \mathbf{m}(\mathbf{X}^*), \mathbf{V}(\mathbf{X}^*))$ , where  $\mathbf{y} = (y_1, \dots, y_N)^T$  and the mean and covariances are, respectively:

$$\mathbf{m}(\mathbf{X}^*) = \mathbf{K}_*^T (\mathbf{K} + \sigma^2 \mathbf{I})^{-1} \mathbf{y}, \quad \mathbf{V}(\mathbf{X}^*) = \mathbf{K}_{*,*} - \mathbf{K}_*^T (\mathbf{K} + \sigma^2 \mathbf{I})^{-1} \mathbf{K}_*. \quad (5)$$

In (5)  $\sigma^2$  is the variance of the Gaussian noise;  $\mathbf{K}_*$  is a  $N \times B$  matrix with the prior covariances between  $\mathbf{f}^*$  and each  $f(\mathbf{x}_i)$ ; and  $\mathbf{K}$  is a  $N \times N$  matrix with the prior covariances among each  $f(\mathbf{x}_i)$ . That is  $K_{ij} = k(\mathbf{x}_i, \mathbf{x}_j)$ , for some covariance function  $k(\cdot, \cdot)$ . Common examples of covariance functions used by GPs are the squared exponential or the Matérn function (Rasmussen, 2003). Finally,  $\mathbf{K}_{*,*}$  is a  $B \times B$  matrix with the prior covariances for each entry in  $\mathbf{f}^*$ .

A GP model has a set of hyper-parameters  $\theta$  that can be adjusted to better fit the data  $\mathcal{D} = \{(\mathbf{x}_i, y_i) | i = 1, \dots, N\}$ . These include the variance of the additive Gaussian noise  $\sigma^2$  and any potential hyper-parameter of the covariance function  $k(\cdot, \cdot)$ . These can be, *e.g.*, the amplitude and the length-scales. Two popular approaches to estimate the values for these hyper-parameters w.r.t the data are: maximizing the log marginal likelihood and approximately computing a posterior distribution for the hyper-parameters. In this work, we will generate approximate samples from the posterior distribution of the GP hyper-parameters using slice sampling as in (Snoek et al., 2012). The predictive distribution of the GP is averaged over these samples.

## 2.2 Batch Bayesian Optimization

Any sequential BO strategy can be transformed into a batch one by iteratively applying the sequential strategy  $B$  times, with  $B$  the size of the batch. To avoid choosing similar points each time, one can simply hallucinate the results of the already chosen pending evaluations (Snoek et al., 2012). For this, the acquisition function is simply updated from  $\alpha(\mathbf{x} | \mathcal{D})$  to  $\alpha(\mathbf{x} | \mathcal{D} \cup (\mathbf{x}_i, \mathbf{h}_i), \forall \mathbf{x}_i \in \mathcal{P})$ , where  $\mathcal{D}$  are the data collected so far,  $\mathcal{P}$  is the set of pending evaluations, and  $\mathbf{h}_i$  denotes the hallucinated evaluation result for the pending evaluation  $\mathbf{x}_i$ . A simple approach is to update the surrogate model after choosing each batch point by setting  $\mathbf{h}_i$  equal to the mean of the predictive distribution given by the GPs (Desautels et al., 2014). Of course, this strategy, which we refer to as parallel sequential, has the disadvantage of requiring the optimization of the acquisition  $B$  times, and also updating the GPs using hallucinated observations. This is expected to lead to extra computational cost than the one of our proposed approach, PPESMOC.

As will be further developed in Section 3, PPESMOC chooses  $\mathbf{X}_{N+1}$  as the batch of points that maximizes the expected reduction in the entropy of the Pareto set in the feasible space,  $\mathcal{X}^*$ . Hence, the acquisition function will now have not only the  $D$  dimensions associated with the dimensions of the input space  $\mathcal{X}$ , but  $B \times D$  dimensions, where  $B$  is the size of the batch. We show in Figure 3 an acquisition function example that takes into account every possible combination value of a batch size of two a one-dimensional problem in the interval  $[0, 1]$ . As we can see, the acquisition function ends up having two dimensions despite being a one-dimensional input space  $\mathcal{X}$ . Of course, this is because the batch size is two. The bigger the batch size the bigger the dimensionality of the acquisition function.

Because of this bigger dimensionality, optimizing the acquisition function is more challenging in the parallel setting than in the sequential setting. The use of approximations based on differences to compute the gradient is no longer feasible. These approximations of the gradient of the acquisition are common in the literature for sequential BO methods. For example, they are used, *e.g.*, in PESMOC to approximate the gradient of the acquisition function and to optimize it (Garrido-Merchán and Hernández-Lobato, 2019). Approximating the gradient in the parallel setting using differences would require  $2BD$  evaluations of the acquisition function, where  $B$  is the batch size and  $D$  the input dimensionality. As the gradient of the acquisition function needs to be computed at each step of its optimization (as when L-BFGS is used for this), it is necessary to compute the exact gradients of the acquisition function w.r.t the inputs. Hopefully, automatic differentiation tools such as Auto-grad can be used for that purpose (Maclaurin et al., 2015).

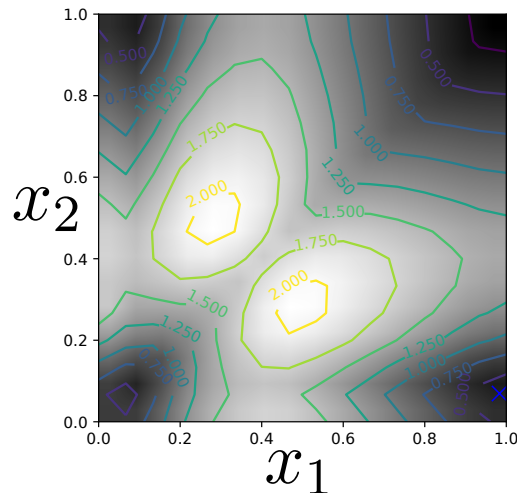


Figure 3: Acquisition function visualization. The batch size is  $B = 2$ . The problem is in one dimension. Each axis corresponds to different values for one of the 2 points in the batch, taking values in the interval  $[0, 1]$ .

### 3 Parallel Predictive Entropy Search for Multi-Objective Bayesian Optimization with Constraints

We now explain in detail the PPESMOC acquisition function. In Section 3.1, we begin by explaining how we can measure the entropy of the minimizer in the classical BO scenario and then describe the generalizations performed to that approach until the parallel constrained multi-objective scenario. We describe in Section 3.2 how PPESMOC can be used to identify such a batch of points by maximizing an acquisition function.



### 3.1 Information-based Acquisition Functions

It is possible to model the minimizer of an optimization problem  $\mathbf{x}^*$  as a random variable (Hennig and Schuler, 2012; Villemonteix et al., 2009; Hernández-Lobato et al., 2014). Hence, we can compute the entropy  $H[p(\mathbf{x}^*)]$  of that random variable with associated probability density function  $p(\mathbf{x}^*)$ . Intuitively, if we want to discover the location of the minimizer  $\mathbf{x}^*$ , we need to minimize the entropy of the location of the extremum  $H[p(\mathbf{x}^*)]$  at every BO iteration. In order to do so, we can measure the amount of information that we have about the minimizer  $\mathbf{x}^*$  of the problem and try to increase it the most at each iteration.

The first acquisition function that used this approach is entropy search (ES) (Villemonteix et al., 2009; Hennig and Schuler, 2012). Specifically, ES, uses the differential entropy of probability distributions to choose the next point to evaluate. Consider  $N$  observations  $\mathcal{D} = \{(\mathbf{x}_i, \mathbf{y}_i)\}_{i=1}^N$  of the black-boxes obtained so far. In particular, we are interested in the point  $\mathbf{x}$ , whose expected evaluation  $y$ , minimizes the expected differential entropy of the conditioned posterior distribution  $\mathbb{E}_{\mathbf{y}}\{H[p(\mathbf{x}^*|\mathcal{D} \cup (\mathbf{x}, y))]\}$  of the optimum  $\mathbf{x}^*$ . That is, the point  $\mathbf{x}$  that maximizes the expected reduction in the differential entropy  $H[\cdot]$  of the posterior for  $\mathbf{x}^*$ . The analytical expression of ES represents this idea. We can write the ES acquisition function  $\alpha(\mathbf{x})$  as:

$$\text{ES}(\mathbf{x}) = H[p(\mathbf{x}^*|\mathcal{D})] - \mathbb{E}_{\mathbf{y}}\{H[p(\mathbf{x}^*|\mathcal{D} \cup \{(\mathbf{x}, y)\})]\}, \quad (6)$$

where the expectation is taken with respect to the predictive distribution  $p(y|\mathcal{D}, \mathbf{x})$  of the black-box function  $f(\mathbf{x})$ . The problem with ES is that the exact computation of the above expression is infeasible in practice. Concretely, computing the probability distribution of the minimizer given the data  $p(\mathbf{x}^*|\mathcal{D})$  is intractable, having to resort to complex approximations (Villemonteix et al., 2009; Hennig and Schuler, 2012).

To circumvent this issue, the PES acquisition function  $\alpha(\mathbf{x})$  is an ES equivalent expression that does not require as many approximations as ES and it is easier to implement (Hernández-Lobato et al., 2014). Specifically, it is possible to perform a trick to convert the analytical expression of ES into another analytical expression that is easier to approximate. This trick is based on the concept of mutual information  $I(X, Y)$  of random variables  $X$  and  $Y$ . In particular, PES uses the fact that mutual information  $I(X, Y)$  is symmetric. Let  $\mathcal{D}$  be the dataset of all evaluations processed by BO until a given iteration  $t$ . Namely,  $\mathcal{D} = \{(\mathbf{x}_i, y_i) | i = 1, \dots, t\}$ . The ES expression in (6) can be equivalently written as the mutual information between  $\mathbf{x}^*$  and  $y$  given  $\mathcal{D}$ , namely,  $\text{ES}(\mathbf{x}) = I(\mathbf{x}^*, y)$ . Since the mutual information  $I(X, Y)$  is a symmetric function, we can swap the roles of  $y$  and  $\mathbf{x}^*$  in the  $\text{ES}(\mathbf{x})$  analytical expression. By doing it so, (6) can be rewritten as:

$$\text{PES}(\mathbf{x}) = H[p(y|\mathcal{D}, \mathbf{x})] - \mathbb{E}_{p(\mathbf{x}^*|\mathcal{D})}[H[p(y|\mathcal{D}, \mathbf{x}, \mathbf{x}^*)]], \quad (7)$$

where  $p(y|\mathcal{D}, \mathbf{x}, \mathbf{x}^*)$  is the conditional predictive distribution for  $y$  at  $\mathbf{x}$  given the observed data  $\mathcal{D}$  and the location  $\mathbf{x}^*$  of the global optimum of the objective function  $f(\mathbf{x})$ . The first term of PES's acquisition function is analytic. The second can be easily approximated. More precisely, the first term of PES  $H[p(y|\mathcal{D}, \mathbf{x})]$  corresponds to the entropy of the GP predictive distribution  $p(y|\mathcal{D}, \mathbf{x})$  of the objective  $f(\mathbf{x})$ , potentially contaminated with noise. This is essentially the entropy of an univariate Gaussian distribution. Nevertheless, the second term of PES in (7) must be approximated by the expectation propagation (EP) algorithm (Minka, 2001; Hernández-Lobato et al., 2014).

The PES acquisition function has been generalized to optimize several objectives via PESMO (Hernández-Lobato et al., 2016), modifying the acquisition function to take into account several objectives. In PESMO, the acquisition function is modified as:

$$\alpha(\mathbf{x}) = H[p(\mathbf{y}|\mathcal{D})] - \mathbb{E}_{p(\mathbf{y}|\mathcal{D}, \mathbf{x})}[H[p(\mathcal{X}^*|\mathcal{D}, \mathbf{x}, \mathcal{X}^*)]], \quad (8)$$

where  $\mathcal{X}^*$  is the Pareto set, which represents the solution to the optimization problem, and  $p(\mathbf{y}|\mathcal{D})$  is the GP predictive distribution for each objective. PES was also generalized to take into account several constraints in PESC (Hernández-Lobato et al., 2015). Here, the notion of feasibility is introduced and a point is only valid if it satisfies all the constraints, that is,  $c_1(\mathbf{x}) \geq 0, \dots, c_C(\mathbf{x}) \geq 0$ .

Every constraint is modeled using a GP and the acquisition function takes into account the predictive distributions of each black-box, including the constraints. As in the other PES acquisition functions, EP is used to approximate the intractable factors. Finally, PESMO and PESC were generalized to tackle multiple objectives under several constraints simultaneously in PESMOC (Garrido-Merchán and Hernández-Lobato, 2019). PESMOC introduced the feasible Pareto set and uses also EP to approximate both the intractable factors of the conditional distributions that appear in the acquisition function. In the next subsection, we present PPESMOC, that generalizes the previous works to the parallel constrained multi-objective scenario. Such an scenario leads to several issues that are addressed in this work. We note that a parallel version of PES for the unconstrained single objective case is described in (Shah and Ghahramani, 2015).

### 3.2 Specification of the Acquisition Function

In this section we describe the proposed acquisition function which leads to the proposed method PPESMOC. Let us define  $\mathbf{X}_{N+1} = \{\mathbf{x}_1, \dots, \mathbf{x}_B\}$  as the batch of  $B$  points where the black-boxes should be evaluated at the next iteration. We choose  $\mathbf{X}_{N+1}$  as the batch of points that maximizes the expected reduction in the entropy of the Pareto set in the feasible space,  $\mathcal{X}^*$ . This is a popular strategy that has shown good empirical results in other sequential optimization settings, including the PESMOC acquisition function (Garrido-Merchán and Hernández-Lobato, 2019). Starting from this idea, the PPESMOC acquisition function is defined as:

$$\alpha(\mathbf{X}) = \mathbb{H}[p(\mathcal{X}^*|\mathcal{D})] - \mathbb{E}_{p(\mathbf{Y}|\mathcal{D}, \mathbf{X})}[\mathbb{H}[p(\mathcal{X}^*|\mathcal{D} \cup (\mathbf{X}, \mathbf{Y}))]], \quad (9)$$

where  $\mathbf{X}$  is the candidate batch of  $B$  points at which to evaluate the black-boxes;  $\mathbf{Y}$  is a matrix with the set of  $B$  noisy evaluations associated to  $\mathbf{X}$ , for each black-box function;  $\mathbb{H}[p(\mathbf{x})] = -\int p(\mathbf{x}) \log p(\mathbf{x}) d\mathbf{x}$  is the differential entropy of the distribution  $p(\mathbf{x})$ ; the expectation is with respect to the posterior predictive distribution of  $\mathbf{Y}$  at the candidate batch  $\mathbf{X}$ , given the data we have observed so far,  $\mathcal{D}$ ; finally,  $p(\mathcal{X}^*|\mathcal{D})$  is the probability distribution of potential Pareto sets  $\mathcal{X}^*$  given the data we have observed so far  $\mathcal{D}$ . Note that the distribution  $p(\mathbf{Y}|\mathcal{D}, \mathbf{X})$ , is given by the product of the predictive distributions of each GP, as indicated in (5), for each black-box function. Namely,  $p(\mathbf{Y}|\mathcal{D}, \mathbf{X}) = \prod_{k=1}^K p(\mathbf{y}_k^o|\mathcal{D}, \mathbf{X}) \prod_{j=1}^J p(\mathbf{y}_j^c|\mathcal{D}, \mathbf{X})$ , where  $\mathbf{y}_k^o$  and  $\mathbf{y}_j^c$  are  $B$ -dimensional vectors with the potential observations of each black-box function, objective or constraint, for each point in the batch  $\mathbf{X}$ . Recall that an independent GP is modeling each black-box function.

Note that (9) involves the entropy of the Pareto set,  $\mathcal{X}^*$ , which can be very difficult to compute. To simplify the computation of the acquisition function, we use the same trick based on the symmetry of mutual information that we described in the previous section. For this, we observe that (9) is the mutual information between  $\mathcal{X}^*$  and  $\mathbf{Y}$ ,  $\mathbb{I}(\mathcal{X}^*, \mathbf{Y})$ . Since the mutual information is symmetric, *i.e.*,  $\mathbb{I}(\mathcal{X}^*, \mathbf{Y}) = \mathbb{I}(\mathbf{Y}, \mathcal{X}^*)$ , we swap the roles of  $\mathcal{X}^*$  and  $\mathbf{Y}$  obtaining:

$$\alpha(\mathbf{X}) = \mathbb{H}[p(\mathbf{Y}|\mathcal{D}, \mathbf{X})] - \mathbb{E}_{p(\mathcal{X}^*|\mathcal{D})}[\mathbb{H}[p(\mathbf{Y}|\mathcal{D}, \mathbf{X}, \mathcal{X}^*)]], \quad (10)$$

where  $p(\mathbf{Y}|\mathcal{D}, \mathbf{X}, \mathcal{X}^*)$  is the predictive distribution for the values of the black-boxes at  $\mathbf{X}$ , given the observed data  $\mathcal{D}$ , and given that the solution of the optimization problem. Namely, the Pareto set in the feasible space, given by  $\mathcal{X}^*$ . Furthermore, the expectation is with respect to  $p(\mathcal{X}^*|\mathcal{D})$ . Namely, the posterior distribution of  $\mathcal{X}^*$  given the data we have observed so far  $\mathcal{D}$ .

Importantly, the first term in (10) can be evaluated analytically since it is just the entropy of the predictive distribution,  $\mathbb{H}[p(\mathbf{Y}|\mathcal{D}, \mathbf{X})]$ , which is a factorizing  $K + J$  dimensional multivariate Gaussian. In particular,

$$\mathbb{H}[p(\mathbf{Y}|\mathcal{D}, \mathbf{X})] = 0.5((K + J)B \log(2\pi e) + \sum_{k=1}^K \log |\mathbf{V}_k^o(\mathbf{X})| + \sum_{j=1}^J \log |\mathbf{V}_j^c(\mathbf{X})|) \quad (11)$$

where  $\mathbf{V}_k^o(\mathbf{X})$  and  $\mathbf{V}_j^c(\mathbf{X})$  are the covariance matrices of the predictive distribution for each black-box function (objective or constraint, respectively) given by (5), plus the corresponding variance of the additive Gaussian noise (*i.e.*,  $\mathbf{I}\sigma^2$ ).

Note that the expectation in (10) can be approximated by a Monte Carlo average. More precisely, one can generate random samples of the black-box functions using a random-feature approximation of each GP, as in Garrido-Merchán and Hernández-Lobato (2019). These samples can then be easily optimized to generate a sample from  $p(\mathcal{X}^*|\mathcal{D})$ . Because the samples of the black-box function are cheap to evaluate, this optimization process has little cost and can be done using, *e.g.*, a grid of points. In practice, we use a finite Pareto set approximated by 50 points. A problem, however, is evaluating the second term that appears in (10). Namely, the entropy of  $p(\mathbf{Y}|\mathcal{D}, \mathbf{X}, \mathcal{X}_s^*)$ , for a particular sample of  $\mathcal{X}^*$ ,  $\mathcal{X}_s^*$ . Such a distribution is intractable. As in the case of PESMOC, we resort to expectation propagation to approximate its value (Minka, 2001).

### 3.3 Approximating the Conditional Predictive Distribution

Assume both  $\mathcal{X}$  and  $\mathcal{X}^*$  have finite size and that  $\mathcal{X}^*$  is known. Later on, we will show how to approximate  $\mathcal{X}$  with a finite size set. Let  $\mathbf{F}$  and  $\mathbf{C}$  be a matrix with the actual objective and constraint values associated to  $\mathcal{X}$ . Then,

$$p(\mathbf{Y}|\mathcal{D}, \mathbf{X}, \mathcal{X}^*) = \int p(\mathbf{Y}|\mathbf{X}, \mathbf{F}, \mathbf{C})p(\mathcal{X}^*|\mathbf{F}, \mathbf{C})p(\mathbf{F}|\mathcal{D})p(\mathbf{C}|\mathcal{D})d\mathbf{F}d\mathbf{C}, \quad (12)$$

where  $p(\mathbf{Y}|\mathbf{X}, \mathbf{F}, \mathbf{C}) = \prod_{b=1}^B \prod_{k=1}^K \delta(y_b^k - f_k(\mathbf{x}_b)) \prod_{j=1}^J \delta(y_b^j - c_j(\mathbf{x}_b))$ , with  $y_b^k$  the evaluation corresponding to the  $k$ -th objective associated to the batch point  $\mathbf{x}_b$ ,  $y_b^j$  the evaluation corresponding to the  $j$ -th constraint associated to the batch point  $\mathbf{x}_b$ ,  $\delta(\cdot)$  a Dirac's delta function and  $B$  the batch size. We have assumed no additive Gaussian noise. In the case of noisy observations, one simply has to replace the delta functions with Gaussians with the corresponding variance,  $\sigma^2$ .

In (12)  $p(\mathbf{F}|\mathcal{D})$  and  $p(\mathbf{C}|\mathcal{D})$  denote the posterior predictive distribution for the objectives and constraints, respectively. Note that we assume independent GPs. Therefore, these distributions factorize across objectives and constraints. They are Gaussians with parameters given in (5). Last, in (12)  $p(\mathcal{X}^*|\mathbf{F}, \mathbf{C})$  is an informal probability distribution that takes value different from zero, only for a valid Pareto set  $\mathcal{X}^*$ . More precisely,  $\mathcal{X}^*$  has to satisfy that  $\forall \mathbf{x}^* \in \mathcal{X}^*$ ,  $\forall \mathbf{x}' \in \mathcal{X}$ ,  $c_j(\mathbf{x}^*) \geq 0$ ,  $\forall j$ , and if  $c_j(\mathbf{x}') \geq 0$ ,  $\forall j$ , then  $\exists k$  s.t.  $f_k(\mathbf{x}^*) < f_k(\mathbf{x}')$ . Namely, each point of the Pareto set has to be better than any other feasible point in at least one of the objectives. These conditions can be summarized as:

$$p(\mathcal{X}^*|\mathbf{F}, \mathbf{C}) \propto \prod_{\mathbf{x}^* \in \mathcal{X}^*} \left( \left[ \prod_{j=1}^J \Phi_j(\mathbf{x}^*) \right] \left[ \prod_{\mathbf{x}' \in \mathcal{X}} \Omega(\mathbf{x}', \mathbf{x}^*) \right] \right) \quad (13)$$

where  $\Phi_j(\mathbf{x}^*) = \Theta(c_j(\mathbf{x}^*))$ , with  $\Theta(\cdot)$  the Heaviside step function, using the convention that  $\Theta(0) = 1$ . Furthermore,

$$\Omega(\mathbf{x}', \mathbf{x}^*) = \left[ \prod_{j=1}^J \Theta(c_j(\mathbf{x}')) \right] \Psi(\mathbf{x}', \mathbf{x}^*) + \left[ 1 - \prod_{j=1}^J \Theta(c_j(\mathbf{x}')) \right] \cdot 1, \quad (14)$$

where  $\Psi(\mathbf{x}', \mathbf{x}^*) = 1 - \prod_{k=1}^K \Theta(f_k(\mathbf{x}^*) - f_k(\mathbf{x}'))$ . The goal of  $\prod_{j=1}^J \Phi_j(\mathbf{x}^*)$  in Equation (13) is to guarantee that every point in  $\mathcal{X}^*$  is feasible. Otherwise,  $p(\mathcal{X}^*|\mathbf{F}, \mathbf{C})$  takes value zero. Similarly,  $\Omega(\mathbf{x}', \mathbf{x}^*)$  can be understood as follows:  $\prod_{j=1}^J \Theta(c_j(\mathbf{x}'))$  checks that  $\mathbf{x}'$  is feasible. If  $\mathbf{x}'$  is infeasible, we do not care and simply multiply everything by 1. Otherwise,  $\mathbf{x}'$  has to be dominated by  $\mathbf{x}^*$ . That is checked by  $\Psi(\mathbf{x}', \mathbf{x}^*)$ . This last factor takes value one if  $\mathbf{x}^*$  dominates  $\mathbf{x}'$  and zero otherwise. Summing up, the r.h.s. of Equation (13) takes value 1 only if  $\mathcal{X}^*$  is a valid Pareto set.

Critically, in Equation (12) all the factors that appear in the r.h.s are Gaussian, except for  $p(\mathcal{X}^*|\mathbf{F}, \mathbf{C})$ . The non-Gaussian factors contained in this distribution are approximated by Gaussians using expectation propagation (EP) (Minka, 2001). Each  $\Phi_j(\mathbf{x}^*)$  factor is approximated by a univariate Gaussian that need not be normalized. Namely,  $\Phi_j(\mathbf{x}^*) \approx \tilde{\mathcal{N}}(c_j(\mathbf{x}^*|\tilde{m}_j^*, \tilde{v}_j^*))$ . The parameters of this Gaussian are tuned by EP. Similarly, each  $\Omega(\mathbf{x}', \mathbf{x}^*)$  is approximated by a

product of  $K$  bivariate Gaussians and  $J$  univariate Gaussians that need not be normalized. That is,

$$\Omega(\mathbf{x}', \mathbf{x}^*) \approx \prod_{k=1}^K \tilde{\mathcal{N}}(\mathbf{v} | \tilde{\mathbf{m}}_k^{\mathbf{x}^*, \mathbf{x}'}, \tilde{\mathbf{V}}_k^{\mathbf{x}^*, \mathbf{x}'}) \prod_{j=1}^J \tilde{\mathcal{N}}(c_j(\mathbf{x}') | \tilde{m}_j^{\mathbf{x}'}, \tilde{v}_j^{\mathbf{x}'}), \quad (15)$$

where  $\mathbf{v} = (f_k(\mathbf{x}^*), f_k(\mathbf{x}'))^T$ . The parameters of these Gaussians are also adjusted by EP. The approximate factors are refined iteratively until their parameters do not change. This ensures that they look similar to the corresponding exact factors.

In our experiments, and when running EP, we replace the set  $\mathcal{X}$  in Equation (13) by a finite set given by  $\{\mathbf{x}_n\}_{n=1}^N \cup \mathbf{X} \cup \mathcal{X}^*$ . Namely, the union of all points that have already being evaluated, the candidate batch  $\mathbf{X}$  and the current Pareto set  $\mathcal{X}^*$  that has been sampled from  $p(\mathcal{X}^* | \mathcal{D})$  when using a Monte Carlo approximation of the expectation in the r.h.s. of Equation (10). These are the input points we have so far. In practice, the  $\Omega(\mathbf{x}', \mathbf{x}^*)$  factors corresponding to  $\mathbf{X}$ , *i.e.*, the batch of points at which to evaluate the acquisition are only refined one time by EP, as in PPSMOC (Garrido-Merchán and Hernández-Lobato, 2019). This ensures that the acquisition function can be quickly evaluated.

### 3.4 PPESMOC’s Acquisition Function

After EP has converged, the conditional predictive distribution in Equation (12) is approximated by replacing each non-Gaussian factor by the corresponding Gaussian approximation obtained by EP. Because all factors are then Gaussian, and the Gaussian family is closed under the product operation, their product can be easily evaluated, resulting in another Gaussian distribution for  $p(\mathbf{Y} | \mathcal{D}, \mathbf{X}, \mathcal{X}^*)$ . Consider  $S$  Monte Carlo samples of  $\mathcal{X}^*$  to approximate the expectation in the r.h.s. of Equation (10). Let  $\mathbf{V}_k^o(\mathbf{X}; s)^{\text{CPD}}$  and  $\mathbf{V}_j^c(\mathbf{X}; s)^{\text{CPD}}$  denote the covariance matrices of the Gaussian approximation of  $p(\mathbf{Y} | \mathcal{D}, \mathbf{X}, \mathcal{X}^*)$  for each objective  $k$  and constraint  $j$ , for sample  $\mathcal{X}_s^*$ . The PPESMOC’s acquisition is simply given by the difference in the entropy before and after conditioning to  $\mathcal{X}^*$ . Namely,

$$\begin{aligned} \alpha(\mathbf{X}) &= \sum_{k=1}^K \log |\mathbf{V}_k^o(\mathbf{X})| + \sum_{j=1}^J \log |\mathbf{V}_j^c(\mathbf{X})| \\ &\quad - \frac{1}{S} \sum_{s=1}^S \left[ \sum_{k=1}^K \log |\mathbf{V}_k^o(\mathbf{X}; s)^{\text{CPD}}| + \sum_{j=1}^J \log |\mathbf{V}_j^c(\mathbf{X}; s)^{\text{CPD}}| \right]. \end{aligned} \quad (16)$$

The cost of computing Equation (16), assuming a constant number of iterations of EP until convergence, is in  $\mathcal{O}((K + J)N^3 + (K + J)B^3)$ , where  $N$  is the number of points observed so far, and  $B$  is the batch size. This cost is a consequence of the GP inference process and having to compute the determinant of matrices of size  $B \times B$ . Importantly, the gradients of Equation (16) w.r.t  $\mathbf{X}$  can be readily computed using automatic differentiation tools such as Autograd (<https://github.com/HIPS/autograd>) (Maclaurin et al., 2015). This is key to guarantee that the acquisition can be optimized using, *e.g.*, quasi-Newton methods (L-BFGS), to find  $\mathbf{X}_{N+1}$ . In our implementation we run EP until convergence one time to approximate the factors corresponding to the observed data  $\mathcal{D}$  and the sampled Pareto set  $\mathcal{X}_s^*$ . These factors are reused and those corresponding to the candidate batch  $\mathbf{X}_{N+1}$  are refined only one time. This saves computational time. We implemented PPESMOC in the software for BO SpearMint. Our implementation is available at [https://github.com/EduardoGarrido90/spearmint\\_ppesmoc](https://github.com/EduardoGarrido90/spearmint_ppesmoc).

Note that (16) includes a sum across each objective and constraint. The consequence is that the acquisition function can be expressed as a sum of one acquisition function per objective and constraint. Namely,  $\alpha(\mathbf{X}) = \sum_{k=1}^K \alpha_k^o(\mathbf{X}) + \sum_{j=1}^J \alpha_j^c(\mathbf{X})$ . This enables the use of PPESMOC decoupled evaluations settings in which one chooses not only where to evaluate the black-boxes, but which black-box to evaluate (Garrido-Merchán and Hernández-Lobato, 2019). For this, one

only has to maximize independently each  $\alpha_k^o(\mathbf{X})$  and  $\alpha_j^c(\mathbf{X})$  to choose then the black-box that leads to the largest expected decrease in the entropy of  $\mathcal{X}^*$ . A decoupled evaluation setting is expected to lead to better optimization results. However, we leave its empirical evaluation for future work.

We illustrate the PPESMOC’s acquisition function in two scenarios of a 1-dimensional problem (for the sake of visualization) with batch size  $B = 2$  in Figure 4 (left) and (right). This problem has two objectives and two constraints. The observations obtained so far are displayed with a blue cross (previous evaluated batch). Each axis corresponds to the potential values (in the interval  $[0, 1]$ ) for each one of the two points in the batch. Figure 4 displays the contour curves of the acquisition function. We remark here some of its properties: (i) It is symmetric w.r.t the diagonal, meaning that the order of the points in the batch does not affect its value. (ii) In the neighborhood of the observed point the acquisition value is low, meaning that the acquisition favors unexplored regions. (iii) In the diagonal the acquisition takes lower values, meaning that it favors diversity in the batch. These are expected properties of a batch BO acquisition function. In these experiments the number of Monte Carlo samples  $S$  is set equal to 10. This is also the number of samples used for the GP hyper-parameters.

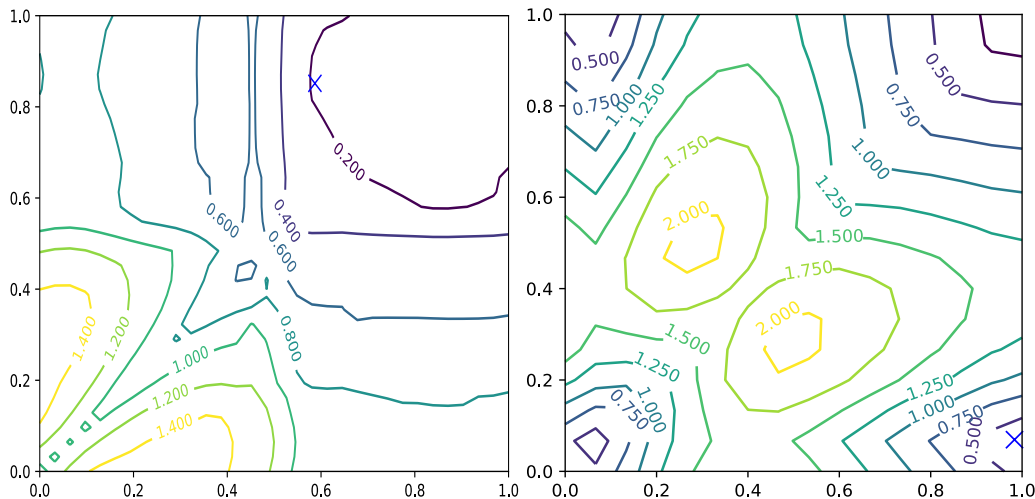


Figure 4: Acquisition function visualization. Each figure corresponds to a different repetition of the optimization problem. The batch size is  $B = 2$ . The problem is in one dimension. Each axis corresponds to different values for one of the 2 points in the batch, taking values in the interval  $[0, 1]$ . Blue crosses show already evaluated locations.

### 3.5 Quality of the Approximation to the Acquisition Function

As described previously, the acquisition function of the proposed method, PPESMOC, is intractable and needs to be approximated. The exact evaluation requires computing an expectation that has no closed form solution and computing the conditional predictive distribution of the probabilistic models given some Pareto set  $\mathcal{X}^*$ . In Section 3.4 we propose to approximate these quantities using Monte Carlo samples and expectation propagation, respectively. In this section we check the accuracy of this approximation to see if it resembles the actual acquisition function. For this, we consider a simple one dimensional problem with a batch of two points, two objectives and one constraint generated from a GP prior. In this simple setting, it is possible to compute a more accurate estimate of the acquisition function using a more expensive sampling technique, combined with a non-parametric estimator of entropy (Singh et al., 2003). More precisely, we discretize the input space and generate a sample of the Pareto set  $\mathcal{X}^*$  by optimizing a sample of the black-box functions. This sample is generated as in the PPESMOC approximation. We then

generate samples of the black-box functions and keep only those that are compatible with  $\lambda^*$  being the solution to the optimization problem. This process is repeated 100,000 times. Then, a non-parametric method is used to estimate the entropy of the predictive distribution at each possible batch of the input space before and after the conditioning. The difference in the entropy at each input location gives a more accurate estimate of the acquisition function of PPESMOC. Of course, this approach is too expensive to be used in practice for solving optimization problems.

Figure 5 shows a comparison between the two estimates of the exact acquisition function. In both plots, the acquisition function values are displayed for all the batch combinations of the input space. The one described above (left, exact) and the one suggested in Section 3.4 (right, approximate). We observe that both estimates of the acquisition function take higher values in regions with high uncertainty and promising predictions. Similarly, both estimates take lower values in regions with low uncertainty. Importantly, both acquisition functions are pretty similar in the sense that they take high and low values in the same regions of the input space. Therefore, both acquisition functions are extremely correlated. This empirical result supports that the approximation proposed in this work is an accurate estimate of the actual acquisition function.

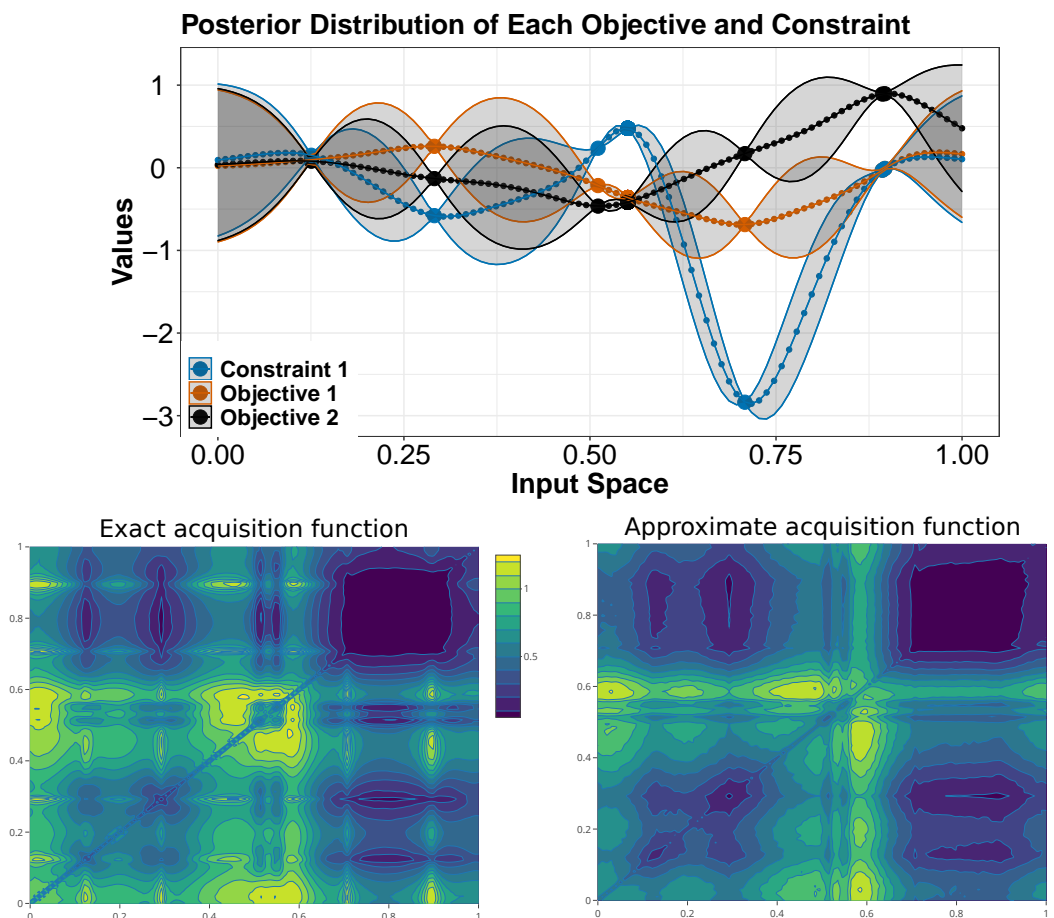


Figure 5: Acquisition function visualization. The batch size is  $B = 2$ . The problem is in one dimension. (top) GP fit to each objective and constraint. (bottom right) Approximate acquisition function. (bottom left) Exact acquisition function computed via expensive Monte Carlo sampling. Each axis corresponds to different values for one of the 2 points in the batch, taking values in the interval  $[0, 1]$ . Note that both acquisitions are low in unfeasible regions.

## 4 Related Work

In this section we review other works from the literature that describe related batch BO methods and BO methods that can address multi-objective problems with constraints. Nevertheless, to our knowledge PPESMOC is the only batch BO method for constrained multi-objective problems. PPESMOC is related to parallel predictive entropy search (PPES) (Shah and Ghahramani, 2015). At each iteration, PPES also selects a batch of points maximizing the expected information gain about the global maximizer of the objective. The computations are also approximated using expectation propagation (EP). The main difference is that PPES is limited to single-objective and un-constrained optimization problems, unlike PPESMOC, which can address multiple objectives and several constraints. This is a non-trivial extension of PPES. In particular, several objectives and constraints require the use of several GPs, not only one. Furthermore, including constraints and several objectives leads to more complicated non-Gaussian factors that need to be approximated using EP. Therefore, the EP update operations of PPESMOC are significantly more complicated than those of PPES. Moreover, the evaluation of the acquisition function in PPES was expensive, making the optimization of the acquisition function unfeasible for batch sizes greater than 3. In order to circumvent this issue, the PPESMOC acquisition function has been optimized via reverse mode differentiation using Autograd (Maclaurin et al., 2015). Additionally, solving multi-objective problems is also more complicated than solving a single-objective problem. In particular, the solution of the later is the Pareto set, a set of potentially infinite size.

Other batch BO methods from the literature include local penalization. This is an heuristic based on an estimate of the Lipschitz constant of the function that penalizes the acquisition function in each neighborhood of already selected points (González et al., 2016). The penalized acquisition function is used to collect batches of points, minimizing the non-parallelizable computational effort. The advantage of this method is that it can be used with arbitrary acquisition functions. A limitation, however, is that it requires to fix the amount of penalization, which depends on the Lipschitz constant of the objective. Such a constant needs to be estimated from data. Another limitation is that this approach computes every point of the batch separately, it transforms the acquisition function based on the previous selected batch points but it does not compute them simultaneously, as in the PPESMOC case, selecting the best possible combination. Furthermore, González et al. (2016) only addresses unconstrained single-objective problems.

Hybrid batch Bayesian optimization dynamically switches, based on the current state, between sequential and batch evaluation policies with variable batch sizes (Azimi et al., 2012). This strategy uses expected improvement as the acquisition function. However, it can only address unconstrained single-objective problems. A batch BO approach can also be implemented via a multi-objective ensemble of multiple acquisition functions (Lyu et al., 2018). In each iteration, a multi-objective optimization of multiple acquisition functions is carried out. A sample of points from the Pareto set is then selected as the batch of points to evaluate. Even though this strategy can address multi-objective problems, it cannot deal with constraints in the optimization process. Other strategies for batch BO that do not address the constrained multi-objective setting include Desautels et al. (2014); Gupta et al. (2018); Kathuria et al. (2016); Daxberger and Low (2017).

Any sequential BO strategy can be transformed into a batch one by iteratively applying the sequential strategy  $B$  times. To avoid choosing similar points each time, one can simply hallucinate the results of the already chosen pending evaluations Snoek et al. (2012). For this, the acquisition function is simply updated from  $\alpha(\mathbf{x}|\mathcal{D})$  to  $\alpha(\mathbf{x}|\mathcal{D} \cup \{\mathbf{x}_i, \mathbf{h}_i\}, \forall \mathbf{x}_i \in \mathcal{P})$ , where  $\mathcal{D}$  are the data collected so far,  $\mathcal{P}$  is the set of pending evaluations, and  $\mathbf{h}_i$  denotes the hallucinated evaluation result for the pending evaluation  $\mathbf{x}_i$ . A simple approach is to update the surrogate model after choosing each batch point by setting  $\mathbf{h}_i$  equal to the mean of the predictive distribution given by the GPs Desautels et al. (2014). Of course, this strategy, which we refer to as parallel sequential, has the disadvantage of requiring the optimization of the acquisition  $B$  times, and also updating the GPs using hallucinated observations. This is expected to lead to extra computational cost than in PPESMOC.

PPESMOC is a generalization of PESMOC, as described in Garrido-Merchán and Hernández-Lobato (2019). PESMOC is the current state-of-the-art for solving constrained multi-objective

BO problems. Nevertheless, PESMOC is a sequential BO method that can only suggest one point at a time to be evaluated. It cannot suggest a batch of points as PPESMOC. PESMOC also works by choosing the next candidate point as the one that is expected to reduce the most the entropy of the Pareto set in the feasible space. The required computations are also approximated using expectation propagation algorithm Minka (2001). Notwithstanding, the extension of PPESMOC over PESMOC is not trivial. In particular, in PPESMOC the acquisition function involves additional non-Gaussian factors (one per each point in the batch) and requires the computation of its gradients. These are not needed in PESMOC as the input dimensionality in that method is smaller, *i.e.*,  $D$  vs.  $B \times D$ . PESMOC approximates the gradient by differences, which is too expensive in the parallel setting.

Bayesian Multi-objective optimization (BMOO) is another strategy for constrained multi-objective BO in the sequential setting Feliot et al. (2017). BMOO is based on the expected hyper-volume improvement acquisition function (EHI) in which the expected increase in the hyper-volume of the Pareto front is computed for each candidate point. The hyper-volume is simply the volume of points in functional space above the Pareto front (*i.e.*, the function values associated to the Pareto set), which is maximized by the actual Pareto set. It is hence a natural measure of utility. When several constraints are introduced in the problem, this criterion boils down to the product of a modified EHI criterion (where only feasible points are considered) and the probability of feasibility, as indicated by the probabilistic models, which are also GPs. BMOO is, however, restricted to the sequential evaluation setting. BMOO was designed originally for a noiseless evaluation setting. However, it has also been shown to be able to solve optimization problems in the noisy setting (Garrido-Merchán and Hernández-Lobato, 2019).

## 5 Experiments

We evaluate the performance of PPESMOC and compare results with two base-lines. Namely, a strategy that chooses at each iteration a random batch of points at which to evaluate the black-boxes. We also compare results with two parallel sequential methods (see Section 4) that use the acquisition function of PESMOC and BMOO, respectively. We refer to these methods as PS\_PESMOC and PS\_BMOO. In each experiment, we report average results and error bars across 100 repetitions. We measure the logarithm of the relative difference between the hyper-volume of the problem’s solution and the hyper-volume of the recommendation provided by each BO method. The solution of the optimization problem is found via exhaustive search in synthetic problems. In real-world problems we use the best recommendation obtained by any method. In each BO method we use a Matérn covariance function for the GPs. The GP hyper-parameters are also sampled from the posterior using 10 slice samples, as in (Snoek et al., 2012). The predictive distribution and acquisition functions are averaged over the samples. In PPESMOC, the number of samples  $S$  of  $\mathcal{X}^*$  is also set to 10 as it was done for PESMOC (Garrido-Merchán and Hernández-Lobato, 2019). In each method, at each iteration, we output a recommendation obtained by optimizing the GP means. For this, we use a grid of points. For the optimization of the acquisition function of each method, we select an initial random point at random and start L-BFGS from it. Finally, we recommend only feasible solutions with high probability as in (Garrido-Merchán and Hernández-Lobato, 2019).

### 5.1 Synthetic Experiments

We compare the performance of each method when the objectives and the constraints are sampled from a GP prior. The problem considered has 2 objectives and 2 constraints in a 4-dimensional input space. We consider a noiseless and a noisy scenario. In this last case, the evaluations are contaminated with Gaussian noise with variance equal to 0.1. We report results for different batch sizes. Namely, 4, 8, 10 and 20 points. We allow for 100 evaluations of each black-box (*i.e.*, a total of 400 evaluations). In the case that the recommendation produced contains an infeasible point, we simply set the hyper-volume of the recommendation equal to zero.



The results obtained are displayed in Figure 6 and Figure 7 for the noiseless and noisy case, respectively. We observe that PPESMOC performs better than PS\_PESMOC and PPESMOC and the other methods in the noiseless setting. The random search strategy gives the worst results followed by PS\_BMOO. In the noisy setting, however, the differences between the methods are less clear and PPESMOC and PS\_BMOO and PS\_PESMOC perform similarly. All of them outperform the random search strategy.

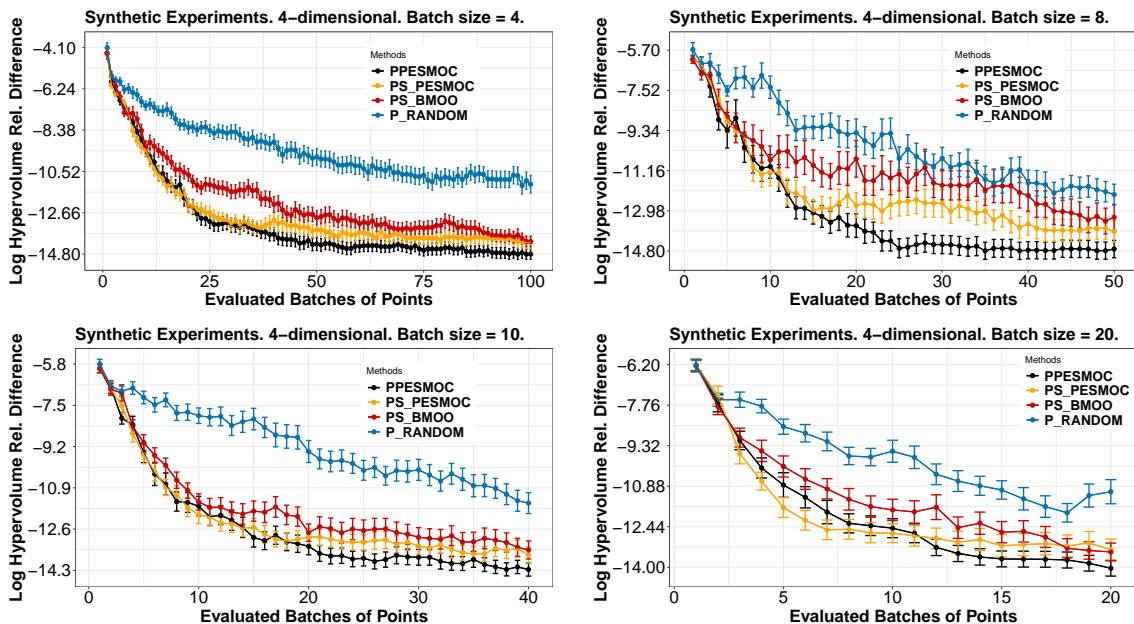


Figure 6: Average results for the synthetic experiments in the noiseless evaluation setting.

The disadvantage of the parallel sequential strategies, PS\_PESMOC and PS\_BMOO, is that they have a bigger computational cost with respect to the batch size  $B$  than PPESMOC. More precisely, they require updating the GP models and optimizing the acquisition  $B$  times. PPESMOC is hence expected to be computationally cheaper for larger batch sizes  $B$ . We add empirical evidence for this claim by showing, in Table 1, the median of the computational time used by each method to determine the next batch of points to evaluate. We note that the parallel sequential strategies are faster for smaller batches of points. This is because the acquisition function is simpler. However, for larger batch sizes, *i.e.*,  $B = 50$ , PPESMOC has a computational time that scales better than the parallel sequential approaches. By contrast, PS\_PESMOC requires, on average, more and more computation time as the batch size  $B$  increases.

Table 1: Median of the time in seconds to choose the next batch of points by PPESMOC and the parallel sequential approaches.

Method	B=4	B=8	B=10	B=20	B=50
PPESMOC	697.3±27.5	913.9±28.1	960.7±27.8	1044.8±30.7	<b>1273.9±30.1</b>
PS_PESMOC	<b>191.3±7.0</b>	<b>346.2±6.1</b>	<b>406.2±6.5</b>	<b>799.8±26.6</b>	1960.3±31.6
PS_BMOO	379.4±12.3	551.7±22.8	594.2±19.9	895.9±27.9	1874.2±42.4

## 5.2 Benchmark Experiments

We carry out extra experiments in which the black-boxes are not sampled from a GP. For this, we consider 6 classical constrained multi-objective optimization problems (Chafekar et al., 2003).

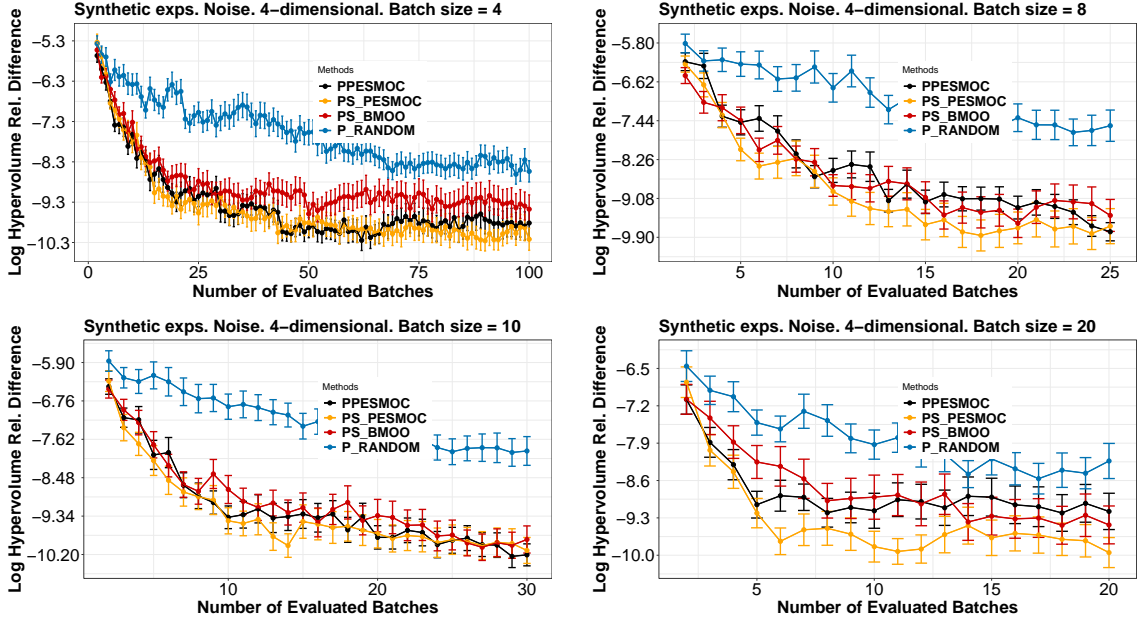


Figure 7: Average results for the synthetic experiments in the noisy evaluation setting.

The analytical expression for the objectives and constraints of each optimization problem are described in the supplementary material. We consider two scenarios. A noiseless scenario and a noisy scenario, where the black-box evaluations are contaminated with additive Gaussian noise. The variance of the noise is set to 1% of the range of potential values of the corresponding black-box. The batch size considered is  $B = 4$ . The average results obtained in these experiments, for each method and each scenario, are displayed in Figure 8, that shows plots of the noiseless case, and Figure 9, showing the noisy setting. We observe that, most of the times, PPESMOC perform similar or better than the other methods, in each scenario, noiseless and noisy, as it was expected.

### 5.3 Real-world Experiments

We compare each method in the task of finding an optimal gradient-boosting ensemble, as in (Garrido-Merchán and Hernández-Lobato, 2019). We consider two objectives: the prediction error of the ensemble and its size. These objectives are conflictive since smaller ensembles will have in general higher error rates and the other way around. We introduce as a constraint of the problem, that the average speed up factor of the classification process given by a dynamic ensemble pruning technique is at least 25% (Hernández-Lobato et al., 2009). We have carefully chosen this value to guarantee that the constraint is active at the optimal solution. The dataset considered is the German credit dataset extracted from the UCI repository (Dua and Graff, 2017). This is a binary classification dataset with 1,000 instances and 20 attributes. The prediction error is measured using 10-fold-cross validation, repeated 5 times. The ensemble size is the logarithm of the sum of the total number of nodes in the trees of the ensemble.

The adjustable parameters of the ensemble are: the number of trees (between 1 and 1,000), the number of random attributes considered for split in each tree (between 1 and 20), the minimum number of samples required to split a node (between 2 and 200), the fraction of randomly selected training data used to build each tree (between 0.5 and 1.0), and the fraction of training instances whose labels are changed after the sub-sampling process (between 0.0 and 0.7).

Table 2 shows the average hyper-volume obtained in this task, for each method, after 100 and 200 evaluations using a batch size of 4. Figure 10 shows also the average Pareto front obtained

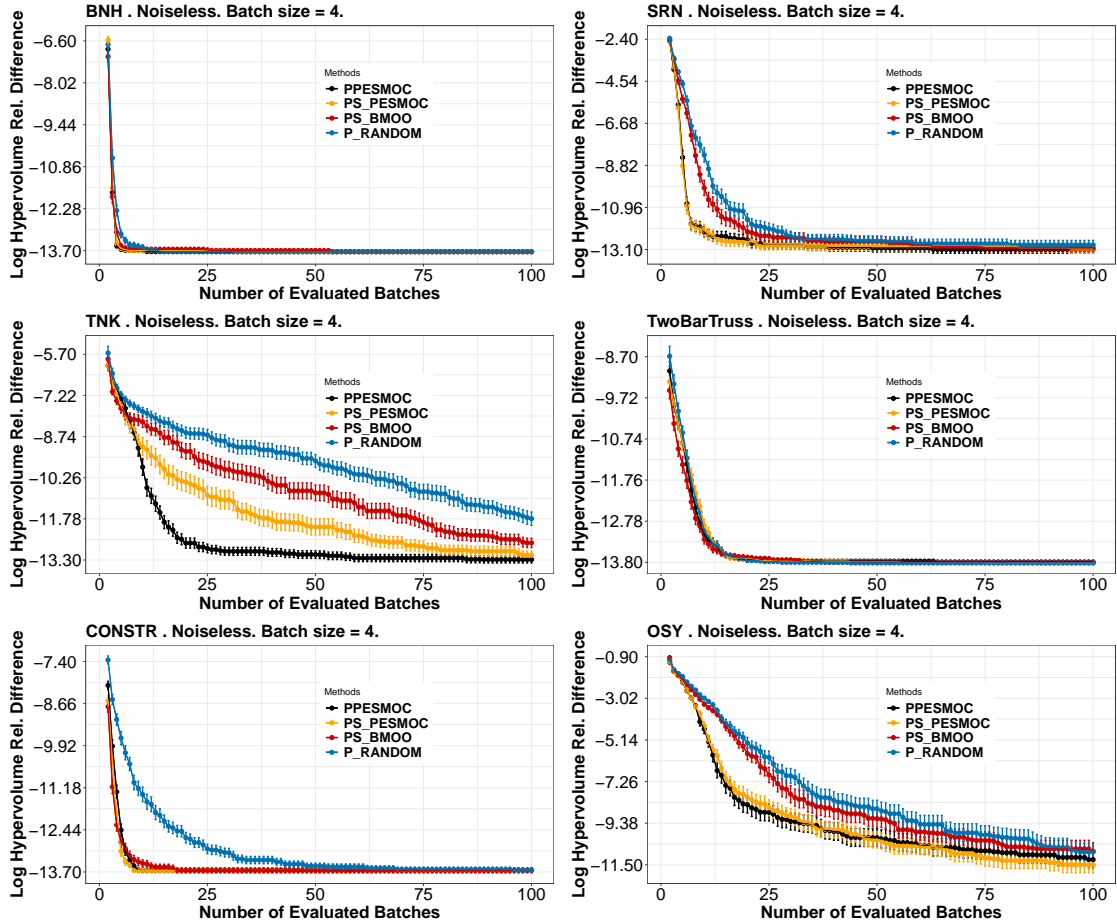


Figure 8: Logarithm of the relative difference between the hyper-volume of the recommendation obtained by each method and the hyper-volume of the actual solution. We report results after each evaluation of the black-box functions. Benchmark functions corrupted by noise.

by each method. The Pareto front is simply given by the objective values associated to the recommendation made by each method. The higher the volume of points that is above this set of points in the objective values the better the performance of a method. We observe that for 100 evaluations PS\_PESMOC is the best strategy closely followed by PPESMOC. However, after 200 evaluations PPESMOC performs better. The random strategy is the worst method and PS\_BMOO and performs slightly worse than PS\_PESMOC.

Table 2: Average hyper-volume in the task of finding an optimal ensemble of trees.

# Eval.	PPESMOC	PS_PESMOC	PS_BMOO	P_RANDOM
100	0.284±0.016	<b>0.287±0.017</b>	0.263±0.020	0.247±0.017
200	<b>0.316±0.006</b>	0.315±0.008	0.298±0.011	0.278±0.010

As described in PESMOC, we also evaluate each method on the task of finding an optimal deep neural network (DNN) on the MNIST dataset (LeCun et al., 2010). The objectives are the prediction error of the DNN on a validation dataset of 10,000 instances (extracted from the original training set) and the time that such a DNN will take for making predictions (normalized with respect to the prediction time of the fastest possible network). These are conflictive objectives in the sense that minimizing the prediction error will often lead to bigger DNN with a bigger

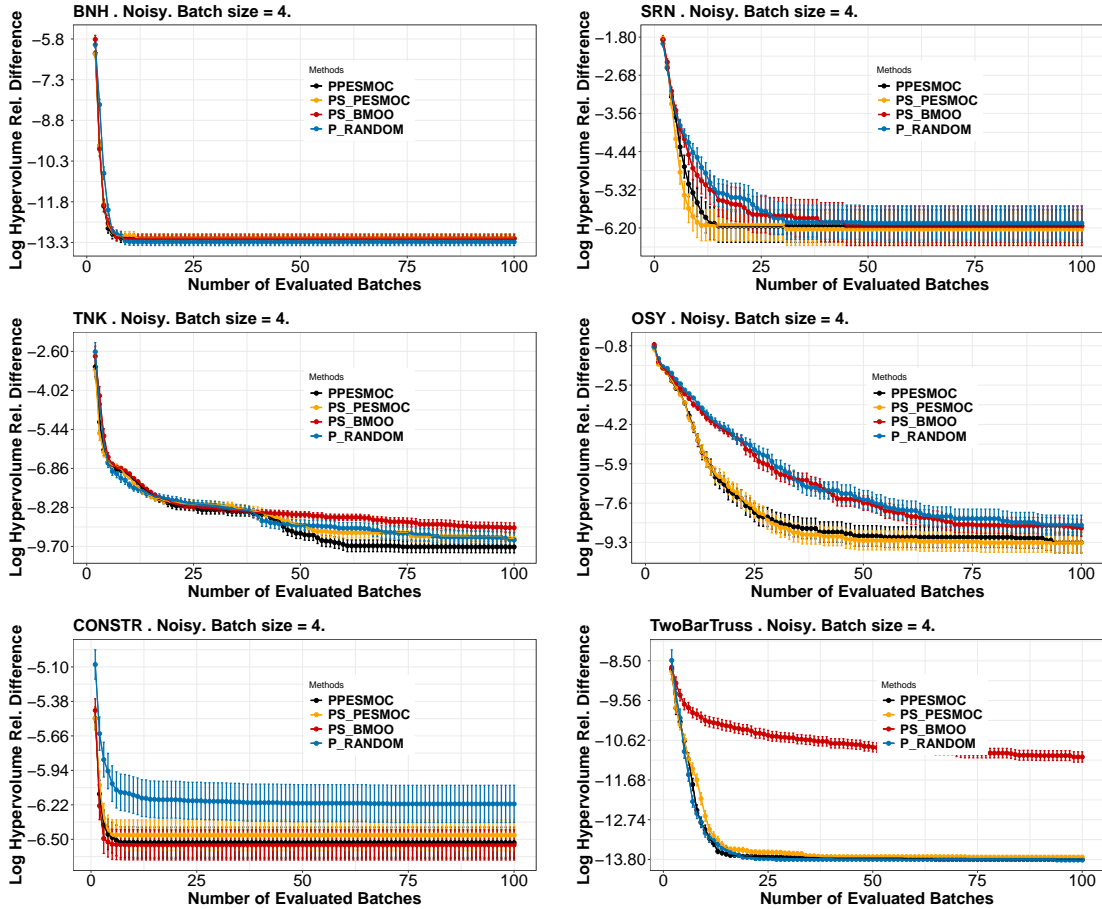


Figure 9: Average results for the problems BNH, SRN, TNK and OSY, CONSTR and TwoBar Truss. Noisy setting.

prediction times. We are also interested in codifying such a DNN into a chip. Thus, we constrain the problem by enforcing that the area of the resulting DNN, after being codified into a chip, is below  $1 \text{ mm}^2$ . We have carefully chosen this value to guarantee that the constraint is active at the optimal solution. To measure the chip area we use the Aladdin simulator, which given a computer program describing the operations of the DNN, outputs an estimate of the area of a chip implementing those operations (Shao et al., 2014). To train the DNN we use the Keras library. Prediction time is normalized by the smallest possible prediction time, which corresponds to a DNN of a single layer with 5 hidden units.

The input parameters to be optimized are: The logarithm of the  $\ell_1$  and  $\ell_2$  weight regularizers; the dropout probability; the logarithm of the initial learning rate; the number of hidden units per layer; and the number of hidden layers. We have also considered two variables that have an impact in the hardware implementation of the DNN. Namely, the logarithm (in base 2) of the array partition factor and the loop unrolling factor.

We report the performance after 60 evaluations using a batch size  $B = 4$ . The DNN is trained using ADAM with the default parameters. The loss function is the cross-entropy. The last layer of the DNN contains 10 units and a soft-max activation function. All other layers use Re-Lu as the activation function. Finally, each DNN is trained during a total of 150 epochs using mini-batches of size 4,000.

The average Pareto front obtained by each method is shown in Figure 11. Time ratio corresponds to the ratio between the time needed for making predictions normalized by the time of the

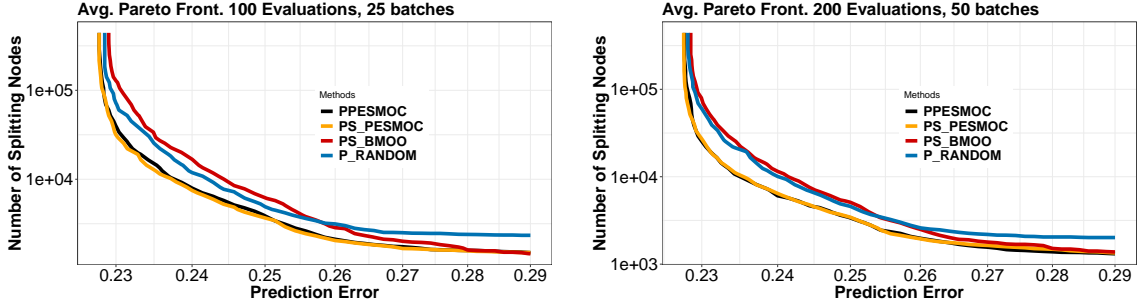


Figure 10: Average Pareto front in the task of finding an optimal ensemble for 100 (left) and 200 evaluations (right).

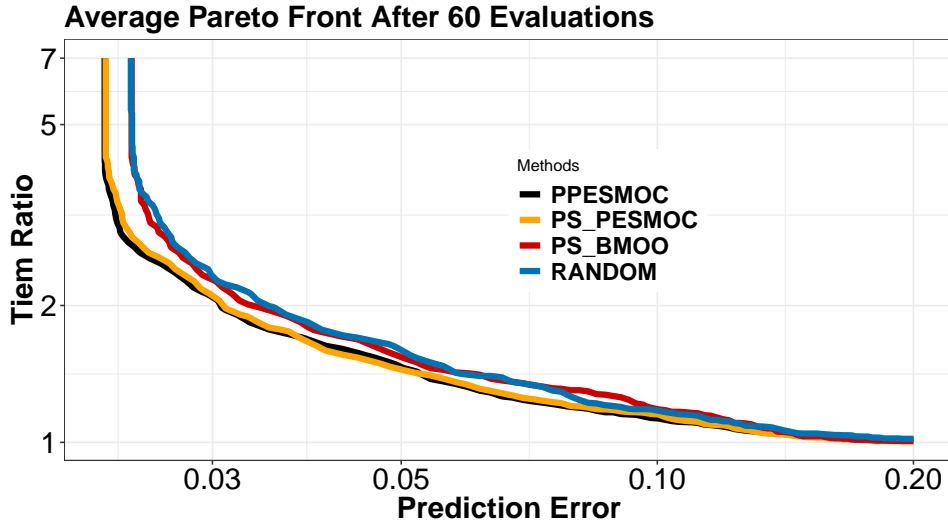


Figure 11: Average Pareto front in the task of finding an optimal neural network for 60 evaluations.

fastest possible network. Table 3 shows the average hyper-volume of each method. Here, PPESMOC outperforms by little PS\_PESMOC. PS\_BMOO gives worse results than PS\_PESMOC and performs almost equal to the random search strategy. We can see in the frontier how the difference between PPESMOC and PS\_PESMOC method is fairly small, however PPESMOC is able to find neural networks with better prediction error for the same prediction time.

Table 3: Avg. hyper-volume of each method in the neural network experiment.

# Eval.	PPESMOC	PS_PESMOC	PS_BMOO	P_RANDOM
60	<b>29.23±0.38</b>	29.09±0.97	28.46±1.54	28.58±0.81

## 6 Conclusions

In this work we have described PPESMOC, the first method to address Bayesian optimization problems with several objectives and constraints in which the black-boxes can be evaluated in parallel. More precisely, PPESMOC suggests, at each iteration, a batch of points at which the ob-

jectives and constraints should be evaluated simultaneously. We have compared the performance of PPESMOC on several optimization problems, including synthetic, benchmark and real-world problems. Furthermore, we have compared results with two simple base-lines. Namely, a random exploration strategy and two methods derived from the literature about sequential Bayesian optimization, PS\_PESMOC and PS\_BMOO. We have observed that PPESMOC performs well in general, giving similar and sometimes better results than PS\_PESMOC and PS\_BMOO. The main advantage is, however, that the PPESMOC acquisition function scales much better with respect to the batch size. Unlike PPESMOC, the sequential strategies require repeating an iterative process as many times as the batch size. This process includes hallucinating observations, re-fitting the underlying GP models, and optimizing a sequential acquisition function. This leads to a prohibitive computational cost for large batch sizes. For small batch sizes, however, these simple strategies are cheap and they give over-all good results that are often similar to those of PPESMOC. Therefore, in that setting, one may consider using them to solve optimization problems with several objectives and constraints in which the evaluations have to be done in parallel.

## Acknowledgments

Authors gratefully acknowledge the use of the facilities of Centro de Computacion Cientifica (CCC) at Universidad Autónoma de Madrid. The authors also acknowledge financial support from Spanish Plan Nacional I+D+i, PID2019-106827GB-I00 /AEI / 10.13039/501100011033.

## References

- Ariizumi, R., Tesch, M., Choset, H., and Matsuno, F. (2014). Expensive multiobjective optimization for robotics with consideration of heteroscedastic noise. In *2014 IEEE/RSJ International Conference on Intelligent Robots and Systems*, pages 2230–2235. IEEE.
- Azimi, J., Jalali, A., and Fern, X. (2012). Hybrid batch Bayesian optimization. *arXiv preprint arXiv:1202.5597*.
- Bergstra, J., Bardenet, R., Bengio, Y., and Kégl, B. (2011). Algorithms for hyper-parameter optimization. In *Advances in neural information processing systems*, pages 2546–2554.
- Brochu, E., Cora, V., and De Freitas, N. (2010). A tutorial on Bayesian optimization of expensive cost functions, with application to active user modeling and hierarchical reinforcement learning. *arXiv preprint arXiv:1012.2599*.
- Chafekar, D., Xuan, J., and Rasheed, K. (2003). Constrained multi-objective optimization using steady state genetic algorithms. In *Genetic and Evolutionary Computation Conference*, pages 813–824.
- Daxberger, E. A. and Low, B. K. H. (2017). Distributed batch Gaussian process optimization. In *International Conference on Machine Learning-Volume 70*, pages 951–960.
- Desautels, T., Krause, A., and Burdick, J. W. (2014). Parallelizing exploration-exploitation trade-offs in Gaussian process bandit optimization. *Journal of Machine Learning Research*, 15:3873–3923.
- Dua, D. and Graff, C. (2017). UCI machine learning repository.
- Feliot, P., Bect, J., and Vazquez, E. (2017). A bayesian approach to constrained single-and multi-objective optimization. *Journal of Global Optimization*, 67(1-2):97–133.
- Feurer, M. and Hutter, F. (2019). Hyperparameter optimization. In *Automated Machine Learning*, pages 3–33. Springer, Cham.

- Garrido-Merchán, E. and Hernández-Lobato, D. (2019). Predictive entropy search for multi-objective Bayesian optimization with constraints. *Neurocomputing*.
- González, J., Dai, Z., Hennig, P., and Lawrence, N. (2016). Batch Bayesian optimization via local penalization. In *Artificial intelligence and statistics*, pages 648–657.
- Gupta, S., Shilton, A., Rana, S., and Venkatesh, S. (2018). Exploiting strategy-space diversity for batch Bayesian optimization. In *International Conference on Artificial Intelligence and Statistics*, pages 538–547.
- Hennig, P. and Schuler, C. (2012). Entropy search for information-efficient global optimization. *Journal of Machine Learning Research*, 13(Jun):1809–1837.
- Hernández-Lobato, D., Hernandez-Lobato, J. M., Shah, A., and Adams, R. P. (2016). Predictive entropy search for multi-objective Bayesian optimization. In *International Conference on Machine Learning*, pages 1492–1501.
- Hernández-Lobato, D., Martínez-Muñoz, G., and Suárez, A. (2009). Statistical instance-based pruning in ensembles of independent classifiers. *IEEE Transactions on Pattern Analysis and Machine Intelligence*, 31:364–369.
- Hernández-Lobato, J. M., Gelbart, M. A., Hoffman, M. W., Adams, R. P., and Ghahramani, Z. (2015). Predictive entropy search for Bayesian optimization with unknown constraints. In *International Conference on Machine Learning*, pages 1699–1707.
- Hernández-Lobato, J. M., Hoffman, M., and Ghahramani, Z. (2014). Predictive entropy search for efficient global optimization of black-box functions. In *Advances in neural information processing systems*, pages 918–926.
- Kathuria, T., Deshpande, A., and Kohli, P. (2016). Batched Gaussian process bandit optimization via determinantal point processes. In *Advances in Neural Information Processing Systems*, pages 4206–4214.
- LeCun, Y., Cortes, C., and Burges, C. (2010). Mnist handwritten digit database. at&t labs.
- Lyu, W., Yang, F., Yan, C., Zhou, D., and Zeng, X. (2018). Batch bayesian optimization via multi-objective acquisition ensemble for automated analog circuit design. In *International conference on machine learning*, pages 3306–3314. PMLR.
- Maclaurin, D., Duvenaud, D., and Adams, R. P. (2015). Autograd: Effortless gradients in numpy. In *ICML 2015 AutoML Workshop*, volume 238, page 5.
- Minka, T. (2001). Expectation propagation for approximate Bayesian inference. In *Proceedings of the Seventeenth conference on Uncertainty in artificial intelligence*, pages 362–369. Morgan Kaufmann Publishers Inc.
- Mockus, J., Tiesis, V., and Zilinskas, A. (1978). The application of bayesian methods for seeking the extremum. *Towards global optimization*, 2(117-129):2.
- Rasmussen, C. (2003). Gaussian processes in machine learning. In *Summer School on Machine Learning*, pages 63–71. Springer.
- Shah, A. and Ghahramani, Z. (2015). Parallel predictive entropy search for batch global optimization of expensive objective functions. In *Advances in Neural Information Processing Systems*, pages 3330–3338.
- Shahriari, B., Swersky, K., Wang, Z., Adams, R., and De Freitas, N. (2015). Taking the human out of the loop: A review of Bayesian optimization. *Proceedings of the IEEE*, 104(1):148–175.

- Shao, Y. S., Reagen, B., Wei, G., and Brooks, D. (2014). Aladdin: A pre-rtl, power-performance accelerator simulator enabling large design space exploration of customized architectures. In *International Symposium on Computer Architecture*, pages 97–108.
- Siarry, P. and Collette, Y. (2003). Multiobjective optimization: principles and case studies.
- Singh, H., Misra, N., Hnizdo, V., Fedorowicz, A., and Demchuk, E. (2003). Nearest neighbor estimates of entropy. *American journal of mathematical and management sciences*, 23:301–321.
- Snoek, J., Larochelle, H., and Adams, R. (2012). Practical Bayesian optimization of machine learning algorithms. In *Advances in neural information processing systems*, pages 2951–2959.
- Villemonteix, J., Vazquez, E., and Walter, E. (2009). An informational approach to the global optimization of expensive-to-evaluate functions. *Journal of Global Optimization*, 44(4):509.